Generating-function approach for bond percolation in hierarchical networks

Takehisa Hasegawa*
Graduate School of Information Science and Technology, The University of Tokyo, 7-3-1 Hongo, Bunkyo-ku, Tokyo, Japan

Masataka Sato† and Koji Nemoto‡
Department of Physics, Graduate School of Science, Hokkaido University, Kita 10-jo Nisi 8-tyome, Sapporo, Japan

(Received 26 April 2010; published 1 October 2010)

We study bond percolations on hierarchical scale-free networks with the open bond probability of the shortcuts $\tilde{p}$ and that of the ordinary bonds p. The system has a critical phase in which the percolating probability P takes an intermediate value $0<P<1$. Using generating function approach, we calculate the fractal exponent ψ of the root clusters to show that ψ varies continuously with $\tilde{p}$ in the critical phase. We confirm numerically that the distribution n_s of cluster size s in the critical phase obeys a power law $n_s \propto s^{-\tau}$, where τ satisfies the scaling relation $\tau=1+\psi^{-1}$. In addition the critical exponent $\beta(\tilde{p})$ of the order parameter varies as $\tilde{p}$, from $\beta \simeq 0.164\,694$ at $\tilde{p}=0$ to infinity at $\tilde{p}=\tilde{p}_c=5/32$.

DOI: 10.1103/PhysRevE.82.046101 PACS number(s): 89.75.Hc, 64.60.aq, 89.65.−s

I. INTRODUCTION

Dynamics on and of complex networks have been one of the focuses of attentions since late 1990s [1–3]. Real networks, e.g., WWW, Internet, food-web, often have complex properties such as scale-free degree distribution [4], small-world property [5], etc., to demand more extensive framework of statistical physics to investigate the interplay between dynamics and such network topology. Many analytical and numerical works about the effects of network topology on processes such as percolation, interacting spin systems, epidemic processes, have been reported [6].

Among these issues, unusual phase transitions of percolations and spin systems on some networks have attracted our current interests [7–16]. For example, the percolations on some growing network models undergo an infinite order transition with a *Berezinskii-Kosterlitz-Thouless (BKT)-like singularity*: (i) the relative size of the largest component vanishes in an essentially singular way at the transition point, so that the transition is of infinite order, and (ii) the mean number n_s of clusters with size s per node (or the cluster size distribution in short) decays in a power-law fashion with s,

$$n_s \propto s^{-\tau}, \tag{1}$$

in a finite region *below* the transition point where no giant component exists [7–11]. A similar nonordered phase with some power-law behavior, *a critical phase*, has also been observed in bond percolations on the enhanced binary tree [17–19], which is one of nonamenable graphs (NAGs) [20,21]. The system on a NAG takes three distinct phases according to the open bond probability p as follows: (i) the nonpercolating phase ($0 \le p \le p_{c1}$) in which only finite size clusters exist, (ii) the critical phase ($p_{c1} \le p \le p_{c2}$) in which there are infinitely many infinite clusters, and (iii) the percolating phase ($p_{c2} \le p \le 1$) in which the system has a unique infinite cluster. Here *infinite cluster* means a cluster whose mass diverges with system size N as N^{ϕ} with $0<\phi\le 1$. To profile the critical phase it is useful to calculate the fractal exponent ψ_{L} defined as $s_{\max} \propto N^{\psi_{\mathrm{L}}}$, where $s_{\max}$ is the mean size of the largest components in the system with N nodes. Note that ψ_{L} corresponds to d_f/d for percolating clusters having the fractal dimension d_f on d-dimensional Euclidean lattices. Recent paper [17] has shown numerically that the above phases are characterized as (i) $\psi_{\mathrm{L}}(p)=0$ for $p<p_{c1}$, (ii) continuously increasing of $\psi_{\mathrm{L}}(p)$ $(0<\psi_{\mathrm{L}}(p)<1)$ with p, where n_s also behaves as Eq. (1) with p-dependent τ satisfying

$$\tau = 1 + \psi_{\mathrm{L}}^{-1}, \tag{2}$$

for $p_{c1}<p<p_{c2}$, and (iii) $\psi_{\mathrm{L}}(p)=1$ for $p>p_{c2}$. The scaling relation (2) indicates that ψ_{L} plays a role of the natural cutoff exponent of n_s as shown in the growing random tree in which $p_{c1}=0$ and $p_{c2}=1$ [11]. In general the growing random networks are considered to have $p_{c1}=0$ with finite p_{c2} [7–10].

There exist other systems having a similar phase. They are in a special class of hierarchical scale-free networks, called (decorated) (u,v)-flower introduced comprehensively in [22,23]. Berker *et al.* [16] have studied bond percolations on the decorated (2,2)-flower by renormalization group (RG) to show the existence of a *critical* phase (as known as the partially ordered phase [24]), where RG flow converges onto the line of nontrivial stable fixed points. But we have little knowledge about physical properties of the critical phase, i.e., how it is critical.

In this paper, we investigate bond percolations on the decorated (2,2)-flower with two different probabilities $\tilde{p}$ and p, which are the open bond probability of the shortcuts and that of the ordinary bonds, respectively. Here we adopt a generating function approach to calculate the fractal exponent, the cluster size distribution, and the order parameter for an arbitrary combination of p and $\tilde{p}$, to reveal a complete picture about the phases of this model. Our calculations show (i) the fractal exponent ψ and β of the order parameter depend on the existing probability $\tilde{p}$ of the shortcuts, and (ii)

*hasegawa@stat.t.u-tokyo.ac.jp
†hijiri@statphys.sci.hokudai.ac.jp
‡nemoto@statphys.sci.hokudai.ac.jp

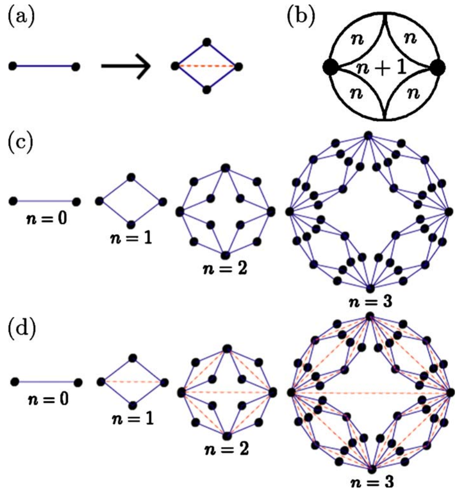

FIG. 1. (Color online) Construction of the (2,2)-flower F_n and the decorated (2,2)-flower $\tilde{F}_n$. (a) Each bond is replaced by two parallel paths consisting of two bonds each at next generation. (b) The flower F_{n+1} of the $n+1$-th generation is obtained by joining four copies of F_n. (c) Realization of F_n with $n=0,1,2,3$. (d) Realization of $\tilde{F}_n$ with $n=0,1,2,3$. $\tilde{F}_n$ is obtained by adding the shortcuts [orange-dashed line in bond replacement (a)] to F_n. The shortcuts are not replaced by others in each iteration.

n_s is a power law at all the point in the critical phase, and its exponent τ also depends on $\tilde{p}$.

The organization of this paper is as follows: In Sec. II, we introduce the (2,2)-flower and the decorated (2,2)-flower, and briefly review the previous studies for the percolation on the flowers [16,22,23]. In Sec. III, we introduce the generating functions, and derive those recursion relations to calculate the order parameter, fractal exponent, and cluster size distribution. The main results are presented in Sec. IV, and Sec. V is devoted to summary.

II. MODEL

In this section we briefly introduce the (2,2)-flower and the decorated (2,2)-flower. The (2,2)-flower F_n of the nth generation is constructed recursively as illustrated in Fig. 1. At $n=0$, the flower F_0 consists of two nodes connected by a bond. Hereafter we call these nodes *roots*. For $n \geq 1$, F_n is obtained from F_{n-1}, such that each existing bond in F_{n-1} is replaced by two parallel paths consisting of two bonds each. The decorated (2,2)-flower $\tilde{F}_n$, a variant of the (2,2)-flower F_n, is given by adding shortcuts to F_n, as illustrated in Fig. 1(d).

The network properties of these two flowers have been reported in [22,23]. The number of nodes N_n of the nth generation is $N_n=2(4^n+2)/3$ and the degree distribution has a scale-free form $P(k) \propto k^{-\gamma}$ with $\gamma=3$ for both flowers. One of the important differences between F_n and $\tilde{F}_n$ appears in those dimensionality. Since the diameter L_n of F_n is $L_n=2^n$, the dimension d of the underlying network defined as $N_n \propto L_n^d$ is 2. On the other hand $\tilde{F}_n$ is known to have small-world property $L_n \sim \ln N_n$ corresponding to $d \sim \infty$. In addition $\tilde{F}_n$ has a

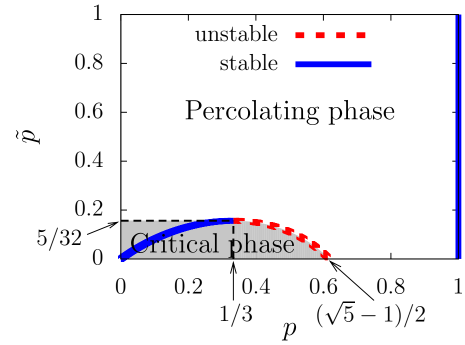

FIG. 2. (Color online) Phase diagram of the bond percolation on the decorated (2,2)-flower [16]. The bold blue-solid and the bold red-dashed lines denote $p^*(\tilde{p})$ (stable fixed point) and $p_c(\tilde{p})$ (unstable fixed point), respectively. The shaded region represents the critical phase.

high clustering coefficient $C \sim 0.820$, in contrast to $C=0$ for F_n.

In the present work we consider the bond percolation on $\tilde{F}_n$ with the open bond probability p of the bonds constituting F_n (the ordinary bonds) and that of the shortcuts $\tilde{p}$ being given independently. The standard bond percolation on F_n and $\tilde{F}_n$ are given by setting $\tilde{p}=0$ and $\tilde{p}=p$, respectively. Note that the latter is also given by setting $p=0$ because $\tilde{F}_n$ with $p=\tilde{p}$ and $\tilde{F}_{n+1}$ with $p=0$ is exactly the same.

The phase diagram is solved exactly by RG technique [16,22]. Let $P^{(n)}$ be a probability that both roots are in the same cluster of a bond configuration on $\tilde{F}_n$ with fixed $\tilde{p}$. The initial value is set to $P^{(0)}=p$. In the large size limit, the system is regarded as percolating if $P := \lim_{n\to\infty} P^{(n)}$ is nonzero. In this sense P or $P^{(n)}$ is called the *percolation* probability. Since $P^{(n)}$ is given recursively as

$$P^{(n+1)} = 1 - (1-\tilde{p})[1-(P^{(n)})^2]^2, \tag{3}$$

one obtains the flow diagram from the solution of the equation (Fig. 2). For $0<\tilde{p}<\tilde{p}_c=5/32$, there are two nonzero stable fixed points, $P=p^*(\tilde{p})<1$ and $P=1$, corresponding to the partially ordered phase and the ordered phase, respectively, and one unstable fixed point between the two giving the phase boundary, $P=p_c(\tilde{p})$. For $\tilde{p}>\tilde{p}_c$, on the other hand, there is only one stable fixed point at $P=1$, so that the system is always percolating.

Two special cases, $\tilde{p}=0$ and $\tilde{p}=p$, were investigated in [22]. Here let us recall their results briefly. For the case of $\tilde{p}=0$, i.e., the standard bond percolation on F_n, Eq. (3) gives the critical point $p_c(\tilde{p}=0)=(\sqrt{5}-1)/2$. A simple RG argu-

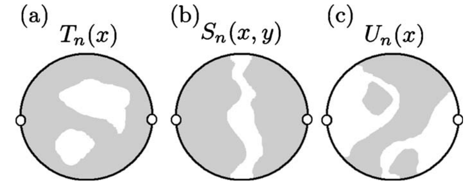

FIG. 3. Schematic for generating functions (a) $T_n(x)$, (b) $S_n(x,y)$, and (c) $U_n(x)$. The open circles represent the root nodes.

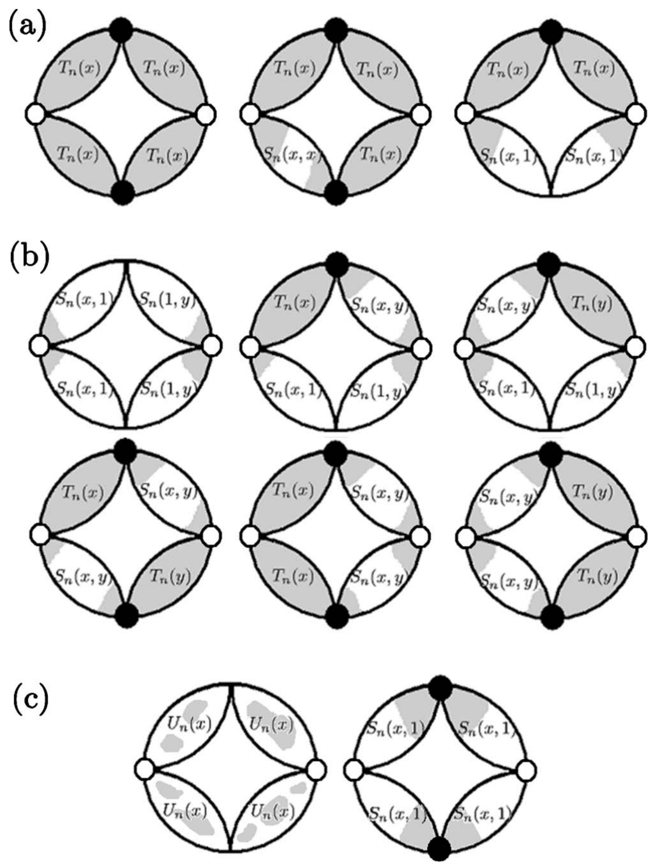

FIG. 4. Possible diagrams contributing to (a) $T_{n+1}(x)$, (b) $S_{n+1}(x,y)$, (c) $U_{n+1}(x)$. The roots (open circles) are not counted in the generating functions, so that nodes connecting two F_ns (closed circles) are taken into account by multiplying x or y. For example the first diagram of (a) represents $x^2T_n^4(x)$ and the fourth diagram of (b) $xyT_n(x)T_n(y)S_n^2(x,y)$.

ment then gives the critical exponents at p_c; the exponent $\beta \simeq 0.164\,694$ of the order parameter, i.e., the fraction of the largest component $P_\infty \sim (p-p_c)^\beta$, and $\nu \simeq 1.63528$ of the correlation length $\xi \sim |p-p_c|^{-\nu}$, which are close to those of the two dimensional regular systems. On the other hand the same argument for $\tilde{p}=p$ gives the infinite order transition, i.e., $\beta \to \infty$.

According to the above definition of percolation the percolating cluster should include both of the root nodes. It is

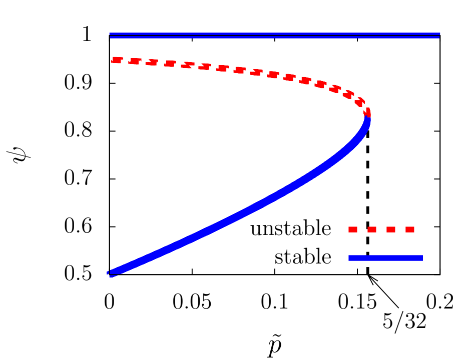

FIG. 5. (Color online) Fractal exponent ψ on the stable fixed points $p^*(\tilde{p})$ (bold blue-solid line) and unstable fixed points $p_c(\tilde{p})$ (bold red-dashed line).

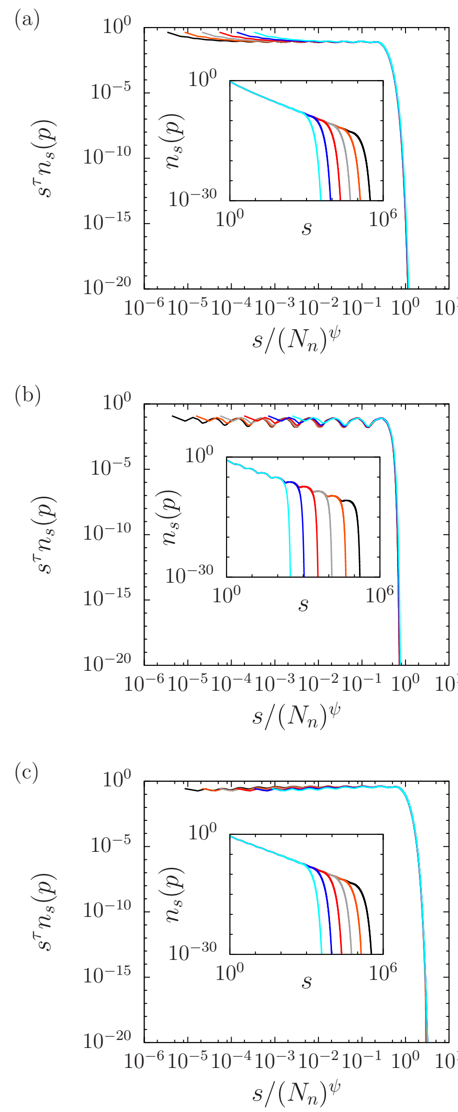

FIG. 6. (Color online) Finite size scaling for cluster size distribution n_s at (a) stable fixed point ($p=0.130\,302$) and (b) unstable fixed point ($p=0.517\,492$), and (c) $p=0.3$, for $\tilde{p}=0.1$. Here ψ and τ in (c) are given by those at the stable fixed point. Insets show raw data of n_s. We set (a) $n=9,10,11,12,13,14$, (b) $n=5,6,7,8,9,10$, and (c) $n=8,9,10,11,12,13$, from left to right.

then convenient to consider the mean size $\langle s_0 \rangle_n$ of the cluster including both roots (referred to as the root cluster) on $\tilde{F}_n$ instead of $s_{\max}(N_n)$ to characterize the criticality,

$$\langle s_0 \rangle_n \propto N_n^\psi, \tag{4}$$

where ψ is the fractal exponent for the root cluster. Note that ψ behaves essentially the same as $\psi_{\rm L}$ for the growing random trees [11].

III. GENERATING FUNCTIONS

In this section we describe how to utilize generating functions to calculate the fractal exponent ψ and the cluster size distribution $n_s(p)$ with $\tilde{p}$ fixed. First let us consider the bond percolation on F_n with open bond probability p with $\tilde{p}=0$.

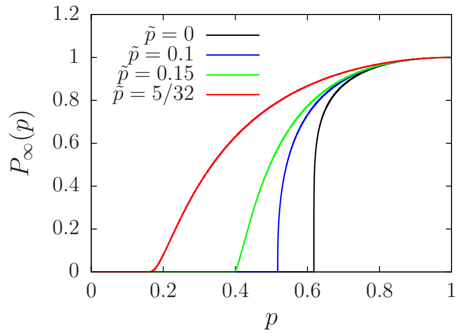

FIG. 7. (Color online) Fraction of the largest components $P_\infty(p)$ on $\tilde{F}_n$ with $\tilde{p}=0,0.1,0.15$, and $5/32(=\tilde{p}_c)$ (from right to left). Here n is taken to $10^6(\gg 1)$.

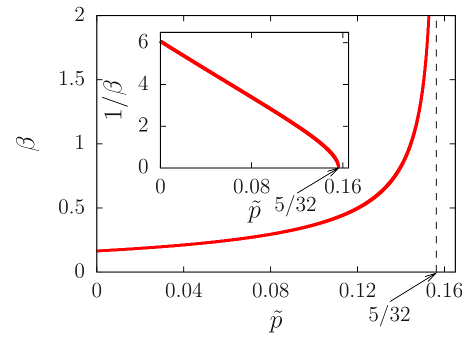

FIG. 8. (Color online) $\tilde{p}$-dependence of the critical exponent β on the phase boundary $p=p_c(\tilde{p})$. Inset shows that of β^{-1}.

We introduce three basic quantities on F_n: the probability $t_k^{(n)}(p)$ that both roots are connected to the same cluster of size k, the probability $s_{k,l}^{(n)}(p)$ that the left (right) root is connected to a cluster of size $k(l)$ but these clusters are not the same, and the mean number $u_k^{(n)}(p)$ of clusters of size k to which neither of the roots is connected. For the sake of convenience the roots are not counted in the cluster size k or l for $t_k^{(n)}(p)$ and $s_{k,l}^{(n)}(p)$. The corresponding generating functions are defined as

$$T_n(x) = \sum_{k=0}^{\infty} t_k^{(n)}(p)x^k, \tag{5a}$$

$$S_n(x,y) = \sum_{k=0}^{\infty}\sum_{l=0}^{\infty} s_{k,l}^{(n)}(p)x^k y^l, \tag{5b}$$

$$U_n(x) = \sum_{k=0}^{\infty} u_k^{(n)}(p)x^k. \tag{5c}$$

The self-similar structure of F_n allows us to obtain the recursion relations for the above generating functions

$$T_{n+1}(x) = x^2T_n^4(x) + 4x^2T_n^3(x)S_n(x,x) + 2xT_n^2(x)S_n^2(x,1), \tag{6a}$$

$$\begin{aligned} S_{n+1}(x,y) &= S_n^2(x,1)S_n^2(1,y) + 2S_n(x,y)S_n(x,1)S_n(1,y) \\ &\quad \times [xT_n(x) + yT_n(y)] + 2xyS_n^2(x,y)T_n(x)T_n(y) \\ &\quad + S_n^2(x,y)[x^2T_n^2(x) + y^2T_n^2(y)], \end{aligned} \tag{6b}$$

$$U_{n+1}(x) = 4U_n(x) + 2xS_n^2(x,1), \tag{6c}$$

as illustrated in Figs. 3 and 4. The initial conditions are given as $T_0(x)=p$, $S_0(x,y)=q=1-p$ and $U_0(x)=0$.

It is convenient to rewrite these recursion formulas in terms of functions of single variable x only. In order to this we introduce new functions $V_n(x)\equiv S_n(x,x)$ and $R_n(x) \equiv S_n(x,1)$ to obtain

$$\begin{aligned} T_{n+1}(x) &= \mathcal{T}[T_n(x),V_n(x),R_n(x),x] \\ &\equiv x^2T_n^4(x) + 4x^2T_n^3(x)V_n(x) + 2xT_n^2(x)R_n^2(x), \end{aligned} \tag{7a}$$

$$\begin{aligned} V_{n+1}(x) &= \mathcal{V}[T_n(x),V_n(x),R_n(x),x] \\ &\equiv R_n^4(x) + 4xT_n(x)V_n(x)R_n^2(x) + 4x^2T_n^2(x)V_n^2(x), \end{aligned} \tag{7b}$$

$$R_{n+1}(x) = \mathcal{R}[T_n(x),R_n(x),x] = R_n^2(x)[1 + xT_n(x)]^2, \tag{7c}$$

$$U_{n+1}(x) = \mathcal{U}[R_n(x),U_n(x),x] \equiv 4U_n(x) + 2xR_n^2(x). \tag{7d}$$

Indeed it is this form that enables us to obtain the solutions for large n numerically.

Now the construction of the recursion relations for $\tilde{F}_n$ with $\tilde{p}$ fixed is straightforward. Let $\tilde{T}_n(x)$, $\tilde{V}_n(x)$, $\tilde{R}_n(x)$, and $\tilde{U}_n(x)$ denote the corresponding generating functions on $\tilde{F}_n$. By using the above formula (7a)–(7d) with these functions one can construct the generating functions $T_{n+1}(x)$, $V_{n+1}(x)$, $R_{n+1}(x)$, and $U_{n+1}(x)$ on the decorated (2,2)-flower of the next generation *without* the shortcut directly connecting the roots,

$$T_{n+1}(x) = \mathcal{T}[\tilde{T}_n(x),\tilde{V}_n(x),\tilde{R}_n(x),x], \tag{8a}$$

$$V_{n+1}(x) = \mathcal{V}[\tilde{T}_n(x),\tilde{V}_n(x),\tilde{R}_n(x),x], \tag{8b}$$

$$R_{n+1}(x) = \mathcal{R}[\tilde{T}_n(x),\tilde{R}_n(x),x], \tag{8c}$$

$$U_{n+1}(x) = \mathcal{U}[\tilde{R}_n(x),\tilde{U}_n(x),x]. \tag{8d}$$

The flower $\tilde{F}_{n+1}$ is made by adding the shortcut to the intermediate one with probability $\tilde{p}$ and one thus obtains

$$\tilde{T}_{n+1}(x) = T_{n+1}(x) + \tilde{p}V_{n+1}(x), \tag{9a}$$

$$\tilde{V}_{n+1}(x) = \tilde{q}V_{n+1}(x), \tag{9b}$$

$$\tilde{R}_{n+1}(x) = \tilde{q}R_{n+1}(x), \tag{9c}$$

$$\tilde{U}_{n+1}(x) = U_{n+1}(x), \tag{9d}$$

where $\tilde{q}=1-\tilde{p}$. The initial conditions are given as $\tilde{T}_0(x)=p$, $\tilde{V}_0(x)=\tilde{R}_0(x)=q$ and $\tilde{U}_0(x)=0$. One can easily check the probability conservation $\widetilde{T}_n(1)+\widetilde{V}_n(1)=1$ by the iteration [Eq. (9)].

Once these generating functions are obtained one can evaluate various quantities of the present interest. For example the percolation probability $P^{(n)}$ is given as

$$P^{(n)}=\widetilde{T}_n(1), \tag{10a}$$

$$Q^{(n)} \equiv 1-P^{(n)}=\widetilde{S}_n(1,1)=\widetilde{V}_n(1)=\widetilde{R}_n(1). \tag{10b}$$

Note that Eq. (3) is reobtained by putting $x=1$ to Eq. (9) and using Eq. (10). The mean number of the root cluster $\langle s_0\rangle_n$ (or the order parameter $P_\infty^{(n)}(p)$) and the cluster size distribution $n_s^{(n)}(p)$ on $\widetilde{F}_n$ are given as

$$\langle s_0\rangle_n=\widetilde{T}'_n(1)+\widetilde{V}'_n(1), \tag{11}$$

$$P_\infty^{(n)}(p)=\frac{\langle s_0\rangle_n}{N_n}=\tau_n+\sigma_n, \tag{12}$$

$$n_s^{(n)}(p)=\frac{\widetilde{u}_s^{(n)}(p)}{N_n}, \tag{13}$$

where the prime denotes the first derivative with respect to x, and we put $\tau_n=\widetilde{T}'_n(1)/N_n$ and $\sigma_n=\widetilde{V}'_n(1)/N_n$.

It is useful to consider the derivatives of recursion relations (9a)–(9c) for evaluating $P_\infty^{(n)}(p)$. By noticing $\widetilde{V}'_n(1)=2\widetilde{R}'_n(1)$ we obtain the recursion relations for τ_n and σ_n as

$$\begin{pmatrix}\sigma_{n+1}\\ \tau_{n+1}\end{pmatrix}=\frac{N_n}{N_{n+1}}\begin{pmatrix}2\widetilde{q}Q^{(n)}(1+P^{(n)})^2 & 4\widetilde{q}(Q^{(n)})^2(1+P^{(n)})\\ 2(1+P^{(n)})[(P^{(n)})^2+\widetilde{p}Q^{(n)}(1+P^{(n)})] & 4[1-\widetilde{q}(Q^{(n)})^2(1+P^{(n)})]\end{pmatrix}\begin{pmatrix}\sigma_n\\ \tau_n\end{pmatrix}+\frac{1}{N_{n+1}}\begin{pmatrix}4\widetilde{q}P^{(n)}(Q^{(n)})^2(1+P^{(n)})\\ 2P^{(n)}[2-P^{(n)}-2\widetilde{q}(Q^{(n)})^2(1+P^{(n)})]\end{pmatrix} \tag{14}$$

$$\simeq\begin{pmatrix}\frac{1}{2}\widetilde{q}Q(1+P)^2 & \widetilde{q}Q^2(1+P)\\ \frac{1}{2}(1+P)[P^2+\widetilde{p}Q(1+P)] & 1-\widetilde{q}Q^2(1+P)\end{pmatrix}\begin{pmatrix}\sigma_n\\ \tau_n\end{pmatrix}\quad(\text{for}\quad n\gg 1), \tag{15}$$

where we recall $P=\lim_{n\to\infty}P^{(n)}$ and $Q=\lim_{n\to\infty}Q^{(n)}$. Note that this expression is an extension of Eq. (31) in [22].

IV. RESULTS

To profile the critical phase we calculate the fractal exponent ψ. In the ordered phase we have trivially $\psi=1$. Otherwise the fixed points $P(<1)$ of the RG Eq. (3) satisfy $\widetilde{q}(1-P)(1+P)^2=1$. The recursion relation (15) is then reduced to

$$\begin{pmatrix}\sigma_{n+1}\\ \tau_{n+1}\end{pmatrix}=\begin{pmatrix}\frac{1}{2} & \alpha\\ \frac{1}{2}P & 1-\alpha\end{pmatrix}\begin{pmatrix}\sigma_n\\ \tau_n\end{pmatrix}, \tag{16}$$

where $\alpha=(1-P)/(1+P)$. By using the largest eigenvalue $\lambda(P)$ of the above matrix,

$$\lambda(P)=\frac{1}{4}[(3-2\alpha)+\sqrt{1-4\alpha(1-2P)+4\alpha^2}], \tag{17}$$

we can calculate the fractal exponent ψ on the fixed points in the same way as [22] does:

$$\psi(P)=1+\frac{\ln\lambda(P)}{\ln 4}. \tag{18}$$

The $\widetilde{p}$-dependence of ψ is shown in Fig. 5. We find that (i) for $\widetilde{p}<\widetilde{p}_c=5/32$, ψ on the (un)stable fixed points increases (decreases) with increasing $\widetilde{p}$, and (ii) for $\widetilde{p}>\widetilde{p}_c$, ψ is equal to one irrespective of both p and $\widetilde{p}$, which means that the system is always in the percolating phase. Let us consider the p-dependence of ψ with $\widetilde{p}<\widetilde{p}_c$ fixed. In the critical phase $[p<p_c(\widetilde{p})]$ the percolation probability $P^{(n)}$ goes to $p^*(\widetilde{p})$ and the exponent $\psi=\psi[p^*(\widetilde{p})]$ is constant in this region. At the critical point $[p=p_c(\widetilde{p})]$ the fixed point is $P=p_c(\widetilde{p})$ itself and thus ψ discontinuously changes to $\psi[p_c(\widetilde{p})]$, and jumps again to one for the percolating phase $[p>p_c(\widetilde{p})]$. This behavior can be also confirmed directly by evaluating the N_n-dependence of $\langle s_0\rangle_n$ numerically (not shown). This result indicates that the probability $\widetilde{p}$ of the shortcuts essentially determines how the system is *critical* in the partially ordered critical phase. On the other hand, for the standard bond percolation on the decorated (2,2)-flower ($\widetilde{p}=p$), the fractal exponent ψ varies continuously with open bond probability p as observed on a NAG [17].

We also evaluate numerically the recursion relations (9a)–(9d) to obtain the cluster size distribution n_s on $\widetilde{F}_n$ given by Eq. (13). We should observe a power-law behavior of n_s in the whole region of the critical phase. To check this behavior we assume a finite size scaling form

$$n_s(N) = s^{-\tau} f(sN^{-\psi}), \tag{19}$$

where ψ is the fractal exponent obtained above and the scaling function $f(x)$ behaves as

$$f(x) \sim \begin{cases} \text{rapidly decaying func.} & \text{for} \quad x \gg 1, \\ \text{constant} & \text{for} \quad x \ll 1, \end{cases} \tag{20}$$

and τ satisfies the scaling relation [11,17]

$$\tau = 1 + \psi^{-1}. \tag{21}$$

As discussed in [11] a plausible argument leads us to the relation as follows: By assuming $n_s \propto s^{-\tau}$ in the critical phase, *a natural cutoff* $s_{\max}$ of the cluster size distribution (a natural cutoff of the degree distribution was introduced in [25]) is given as

$$N\int_{s_{\max}}^{\infty} n_s ds \simeq 1 \rightarrow s_{\max} \propto N^{1/(\tau-1)}. \tag{22}$$

Here we emphasize that $s_{\max}$ plays just a role of characteristic cutoff of the distribution and does not need to be strictly the mean size of the largest clusters. In this sense we can replace the fractal exponent ψ_{L} of $s_{\max}$ with ψ of $\langle s_0 \rangle$, so that the relation (21) follows. Indeed the largest cluster *not* containing the roots is expected to the one containing the topmost (or, equivalently, bottom-most) node in the right figure of Fig. 4(c) contributing the second term of Eq. (6c). The mean size of the cluster is proportional to $\tilde{V}_n'(1)$ and so to $\langle s_0 \rangle$. Therefore one can conclude that the characteristic size grows with N not faster than N^{ψ}.

Our finite size scaling for n_s is indeed well fitted on both stable and unstable fixed points as shown in Fig. 6. Note that for the sake of Eq. (21) no fitting parameter remains. The scaling also works at any p in the critical phase [Fig. 6(c)], but the convergence is not so rapid as on the fixed points.

Finally, we iterate Eq. (15) numerically to obtain the order parameter $P_{\infty}^{(n)}(\tilde{p})$ on $\tilde{F}_n$. The result for $n=10^6$ is shown in Fig. 7. The initial growth of the order parameter becomes moderate with increasing $\tilde{p}$. To examine the critical exponent β on the phase boundary $p=p_c(\tilde{p})$, we follow the scaling argument in [22] to obtain

$$\beta(\tilde{p}) = -\frac{\ln \lambda[p_c(\tilde{p})]}{\ln \Lambda[p_c(\tilde{p})]}, \tag{23}$$

where

$$\Lambda(P) = \left.\frac{\partial P^{(n+1)}}{\partial P^{(n)}}\right|_P = 4\tilde{q}P(1-P^2) = 2(1-\alpha). \tag{24}$$

Figure 8 shows the $\tilde{p}$-dependence of β. We find that β increases continuously with $\tilde{p}$, from β=0.164 694 at $\tilde{p}$=0 to $\beta=\infty$ at $\tilde{p}=\tilde{p}_c$=5/32. At $\tilde{p}=\tilde{p}_c$ we expand Eq. (3) near $p_c(\tilde{p}_c)$=1/3 to obtain

$$\Delta P^{(n+1)} \simeq \Delta P^{(n)} + \frac{9}{8}(\Delta P^{(n)})^2, \tag{25}$$

where $\Delta P^{(n)}=P^{(n)}-p_c(\tilde{p}_c)$. We can estimate the solution for small $\Delta P^{(0)}=p-p_c(\tilde{p}_c)>0$ as

$$\Delta P^{(n)} \simeq \Delta P^{(0)} + \frac{9n}{8}(\Delta P^{(0)})^2, \tag{26}$$

which is correct as long as the second term in the rhs is much less than the first one, or equivalently, n is much less than $n^* \simeq 1/\Delta P^{(0)}=|p-p_c|^{-1}$. For $n \gtrsim n^*$, $P^{(n)}$ goes to 1 rapidly and so we obtain

$$P_{\infty} \sim \lambda^{n^*} \sim \exp\left(-\frac{\text{const.}}{p-p_c}\right), \tag{27}$$

where $\lambda=\lambda[p_c(\tilde{p}_c)]$ given by Eq. (17). We thus find an essential singularity in the order parameter at $\tilde{p}=\tilde{p}_c$.

Note that β is apparently related to ψ through $\lambda[p_c(\tilde{p})]$ as shown in [22] [see Eqs. (18) and (23)]. It is, however, not the case in the (off-boundary) critical phase where the nontrivial stable fixed points $p^*(\tilde{p})$ dominate the criticality while the order parameter vanishes there.

V. SUMMARY

We have investigated bond percolations on the decorated (2,2)-flower with two different probabilities p and $\tilde{p}$. Our generating function approach has revealed that the system is in the critical phase for $p<p_c(\tilde{p})$ and $\tilde{p}<\tilde{p}_c$=5/32. We have evaluated the fractal exponent ψ and confirmed the power-law behavior of n_s in the critical phase as well as those dependence on p and $\tilde{p}$ and the validity of the scaling relation $\tau=1+\psi^{-1}$.

We have also examined the critical exponent β in the percolating phase and found that β also varies as $\tilde{p}$ from $\beta \simeq 0.164\,694$ at $\tilde{p}$=0, where the network is two-dimensional-like, to $\beta=\infty$ at $\tilde{p}=\tilde{p}_c$, where the dimensionality of the underlying network is infinite.

It is only at $\tilde{p}=\tilde{p}_c$ that the percolation on the decorated (2,2)-flower shows an infinite order transition with the BKT-like singularity as percolations on growing networks do [7–10]. The finiteness of β for $\tilde{p}<\tilde{p}_c$ suggests that the existence of some critical phase adjacent to the *normal* ordered phase is not enough for the network to have such an essential singularity in the order parameter and thus an infinite order phase transition. At present we have none of the key to reveal necessary conditions for the existence of the BKT-like singularity. Further study would be required to clarify the relation between these interesting properties of the phase transition.

ACKNOWLEDGMENTS

The authors thank Tomoaki Nogawa for helpful discussions.

[1] R. Albert and A.-L. Barabási, Rev. Mod. Phys. **74**, 47 (2002).
[2] M. E. J. Newman, SIAM Rev. **45**, 167 (2003).
[3] S. Boccaletti, V. Latora, Y. Moreno, M. Chavez, and D.-U. Hwang, Phys. Rep. **424**, 175 (2006).
[4] A.-L. Barabási and R. Albert, Science **286**, 509 (1999).
[5] D. J. Watts and S. H. Strogatz, Nature (London) **393**, 440 (1998).
[6] S. N. Dorogovtsev, A. V. Goltsev, and J. F. F. Mendes, Rev. Mod. Phys. **80**, 1275 (2008).
[7] D. S. Callaway, J. E. Hopcroft, J. M. Kleinberg, M. E. J. Newman, and S. H. Strogatz, Phys. Rev. E **64**, 041902 (2001).
[8] S. N. Dorogovtsev, J. F. F. Mendes, and A. N. Samukhin, Phys. Rev. E **64**, 066110 (2001).
[9] L. Zalányi, G. Csárdi, T. Kiss, M. Lengyel, R. Warner, J. Tobochnik, and P. Érdi, Phys. Rev. E **68**, 066104 (2003).
[10] M. Coulomb and S. Bauer, Eur. Phys. J. B **35**, 377 (2003).
[11] T. Hasegawa and K. Nemoto, Phys. Rev. E **81**, 051105 (2010).
[12] M. Bauer, S. Coulomb, and S. N. Dorogovtsev, Phys. Rev. Lett. **94**, 200602 (2005).
[13] E. Khajeh, S. N. Dorogovtsev, and J. F. F. Mendes, Phys. Rev. E **75**, 041112 (2007).
[14] M. Hinczewski and A. N. Berker, Phys. Rev. E **73**, 066126 (2006).
[15] T. Hasegawa and K. Nemoto, Phys. Rev. E **80**, 026126 (2009).
[16] A. N. Berker, M. Hinczewski, and R. R. Netz, Phys. Rev. E **80**, 041118 (2009).
[17] T. Nogawa and T. Hasegawa, J. Phys. A **42**, 145001 (2009).
[18] T. Nogawa and T. Hasegawa, J. Phys. A **42**, 478002 (2009).
[19] S. K. Baek, P. Minnhagen, and B. J. Kim, J. Phys. A **42**, 478001 (2009).
[20] R. Lyons, J. Math. Phys. **41**, 1099 (2000).
[21] R. H. Schonmann, Commun. Math. Phys. **219**, 271 (2001).
[22] H. D. Rozenfeld and D. ben-Avraham, Phys. Rev. E **75**, 061102 (2007).
[23] H. D. Rozenfeld, S. Havlin, and D. ben Avraham, New J. Phys. **9**, 175 (2007).
[24] S. Boettcher, J. L. Cook, and R. M. Ziff, Phys. Rev. E **80**, 041115 (2009).
[25] S. N. Dorogovtsev, J. F. F. Mendes, and A. N. Samukhin, Phys. Rev. E **63**, 062101 (2001).